Ocean Modelling 106 (2016) 58–67

Contents lists available at ScienceDirect

Ocean Modelling

journal homepage: www.elsevier.com/locate/ocemod

Development of a Godunov-type model for the accurate simulation of dispersion dominated waves

Scott F. Bradford

Naval Research Laboratory, 4555 Overlook Ave. SW, Washington DC 20375, United States

ARTICLE INFO

Article history:
Received 7 October 2015
Revised 6 September 2016
Accepted 15 September 2016
Available online 16 September 2016

Keywords:
Navier–Stokes equations
Numerical models
Flow simulation
Wave propagation

ABSTRACT

A new numerical model based on the Navier–Stokes equations is presented for the simulation of dispersion dominated waves. The equations are solved by splitting the pressure into hydrostatic and non-hydrostatic components. The Godunov approach is utilized to solve the hydrostatic flow equations and the resulting velocity field is then corrected to be divergence free. Alternative techniques for the time integration of the non-hydrostatic pressure gradients are presented and investigated in order to improve the accuracy of dispersion dominated wave simulations. Numerical predictions are compared with analytical solutions and experimental data for test cases involving standing, shoaling, refracting, and breaking waves.

Published by Elsevier Ltd.

1. Introduction

Numerical models that solve the Navier–Stokes equations and track the free surface location using the Volume-of-Fluid (VOF) method Hirt and Nichols (1981) have successfully simulated near shore wave transformation including breaking (Lin and Liu, 1998; Bradford, 2000). In this approach, the free surface is tracked by monitoring the movement of water in and out of stationary computational cells, which allows for the simulation of arbitrary air-water interfaces. However, these models are computationally intensive and yield solutions that are often more detailed than necessary for many applications.

An alternative group of models track the free surface by utilizing the depth integrated incompressibility constraint (Stansby and Zhou, 1998; Lin and Li, 2002; Stelling and Zijlema, 2003; Bradford, 2005; Ma et al., 2012) or the kinematic free surface boundary condition (Li and Fleming, 2001; Li, 2008). These models typically employ a vertical grid transformation using bottom and free surface tracking coordinates. This approach requires fewer computational cells in the vertical direction than the VOF-based models, which allows for larger scale simulations of coastal wave transformation. However, the ability to simulate the curling over of a wave crest or fluid detachment due to splashing or plunging is lost. Despite this limitation, Bradford (2011) demonstrated that this approach can accurately simulate important aspects of the surf zone including wave height transformation and undertow.

Waves with relatively short lengths and traveling in relatively deep water are typically dominated by frequency dispersion. Accurate simulation of such waves requires greater vertical grid resolution than is required for the accurate simulation of long waves in shallow water. This is particularly true for models that employ a fractional step or projection approach in which the non-hydrostatic pressure is integrated in time with a first order accurate method such as the model presented in Bradford (2011). In this study, two techniques for improving the accuracy of the model presented in Bradford (2011) when simulating dispersion dominated waves are proposed and evaluated. Model predictions are compared with analytical solutions and experimental data.

2. Governing equations

The model is based on the incompressible, Reynolds averaged, Navier–Stokes equations in which the pressure is split into hydrostatic and non-hydrostatic components. Lateral diffusion terms have also been neglected. The governing equations are transformed vertically from z space to σ space via the following transformation (Phillips, 1957),

$$\sigma = \frac{z - h}{D} \tag{1}$$

where h is the free surface elevation and D is the total water depth.

Furthermore, the equations are transformed from x and y space via a curvilinear transformation to ξ and η space such that the grid size in each of the ξ and η directions is one. In this coordinate

E-mail address: scott.bradford@nrl.navy.mil

http://dx.doi.org/10.1016/j.ocemod.2016.09.008
1463-5003/Published by Elsevier Ltd.

system, the momentum equations are

$$\frac{\partial \mathbf{U}}{\partial t}+\frac{1}{A}\left(\frac{\partial \mathbf{F}}{\partial \xi}+\frac{\partial \mathbf{G}}{\partial \eta}\right)+\frac{\partial}{\partial \sigma}\left(\mathbf{H}-\frac{\nu}{D^2}\frac{\partial \mathbf{U}}{\partial \sigma}\right)=\mathbf{Z}+\mathbf{P} \tag{2}$$

where $\mathbf{U}=(Du \quad Dv \quad Dw)^T$, A is the projected area of a computational cell in $x-y$ space, ν is the eddy viscosity. Note that lateral diffusion has been neglected because it has been found that these terms have no significant impact on predictions of the surface elevation and undertow in breaking and non-breaking waves (Bradford, 2011; Ma et al., 2012). The fluxes are

$$\mathbf{F}=\begin{pmatrix} DUu+\frac{1}{2}gD^2A\xi_x \\ DUv+\frac{1}{2}gD^2A\xi_y \\ DUw \end{pmatrix} \quad \mathbf{G}=\begin{pmatrix} DVu+\frac{1}{2}gD^2A\eta_x \\ DVv+\frac{1}{2}gD^2A\eta_y \\ DVw \end{pmatrix} \quad \mathbf{H}=\begin{pmatrix} Wu \\ Wv \\ Ww \end{pmatrix} \tag{3}$$

where

$$U=(u\xi_x+v\xi_y)A$$

$$V=(u\eta_x+v\eta_y)A$$

$$W=D(\sigma_t+u\sigma_x+v\sigma_y)+w \tag{4}$$

ξ_x, ξ_y, η_x, and η_y denote the lateral (time invariant) grid transformation metrics. The terms σ_t, σ_x, and σ_y are the time-varying grid transformation metrics.

The source terms are defined as

$$\mathbf{Z}=\begin{pmatrix} \frac{g}{2}\left(\frac{\partial z_b^2}{\partial \xi}\xi_x+\frac{\partial z_b^2}{\partial \eta}\eta_x\right)-gh\left(\frac{\partial z_b}{\partial \xi}\xi_x+\frac{\partial z_b}{\partial \eta}\eta_x\right) \\ \frac{g}{2}\left(\frac{\partial z_b^2}{\partial \eta}\xi_y+\frac{\partial z_b^2}{\partial \eta}\eta_y\right)-gh\left(\frac{\partial z_b}{\partial \eta}\xi_y+\frac{\partial z_b}{\partial \eta}\eta_y\right) \\ 0 \end{pmatrix} \tag{5}$$

$$\mathbf{P}=\begin{pmatrix} -D\left(\frac{\partial p}{\partial \xi}\xi_x+\frac{\partial p}{\partial \eta}\eta_x+\frac{\partial p}{\partial \sigma}\sigma_x\right) \\ -D\left(\frac{\partial p}{\partial \xi}\xi_y+\frac{\partial p}{\partial \eta}\eta_y+\frac{\partial p}{\partial \sigma}\sigma_y\right) \\ -\frac{\partial p}{\partial \sigma} \end{pmatrix} \tag{6}$$

The variable z_b denotes the bottom elevation and p is the kinematic pressure.

The incompressibility constraint is

$$\frac{\partial D}{\partial t}+\frac{1}{A}\left(\frac{\partial (DU)}{\partial \xi}+\frac{\partial (DV)}{\partial \eta}\right)+\frac{\partial W}{\partial \sigma}=0 \tag{7}$$

Eq. (7) is vertically integrated to yield

$$A\frac{\partial D}{\partial t}+\frac{\partial (D\bar{U})}{\partial \xi}+\frac{\partial (D\bar{V})}{\partial \eta}=0 \tag{8}$$

where $\bar{U}$ and $\bar{U}$ denote the depth averaged velocities defined as

$$\bar{U}=\int_{-1}^{0}Ud\sigma \qquad \bar{V}=\int_{-1}^{0}Vd\sigma \tag{9}$$

The primitive, inviscid form of the momentum equations are also used and are written as

$$\frac{\partial u}{\partial t}+\frac{1}{A}\left(U\frac{\partial u}{\partial \xi}+V\frac{\partial u}{\partial \eta}\right)+\frac{W}{D}\frac{\partial u}{\partial \sigma}=-g\left(\xi_x\frac{\partial h}{\partial \xi}+\eta_x\frac{\partial h}{\partial \eta}\right) -\frac{\partial p}{\partial \xi}\xi_x-\frac{\partial p}{\partial \eta}\eta_x-\frac{\partial p}{\partial \sigma}\sigma_x \tag{10}$$

$$\frac{\partial v}{\partial t}+\frac{1}{A}\left(U\frac{\partial v}{\partial \xi}+V\frac{\partial v}{\partial \eta}\right)+\frac{W}{D}\frac{\partial v}{\partial \sigma}=-g\left(\xi_y\frac{\partial h}{\partial \xi}+\eta_y\frac{\partial h}{\partial \eta}\right) -\frac{\partial p}{\partial \xi}\xi_y-\frac{\partial p}{\partial \eta}\eta_y-\frac{\partial p}{\partial \sigma}\sigma_y \tag{11}$$

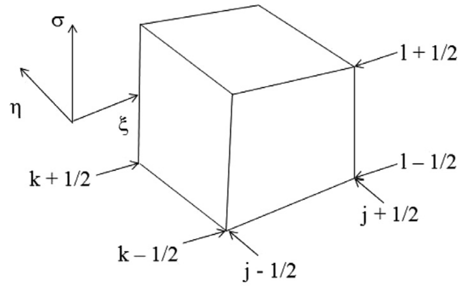

Fig. 1. Sketch of a computational cell.

$$\frac{\partial w}{\partial t}+\frac{1}{A}\left(U\frac{\partial w}{\partial \xi}+V\frac{\partial w}{\partial \eta}\right)+\frac{W}{D}\frac{\partial w}{\partial \sigma}=-\frac{1}{D}\frac{\partial p}{\partial \sigma} \tag{12}$$

The primitive form of Eq. (8) is

$$\frac{\partial D}{\partial t}+\bar{U}\frac{\partial D}{\partial \xi}+\bar{V}\frac{\partial D}{\partial \eta}+D\left(\frac{\partial \bar{U}}{\partial \xi}+\frac{\partial \bar{V}}{\partial \eta}\right)=0 \tag{13}$$

The Mellor–Yamada 2.5 level turbulence model (Mellor and Yamada, 1982; Galperin et al., 1988) is used to compute ν. This turbulence closure model yielded results similar to those obtained with the Renormalized Group turbulence closure model coupled with a Volume of Fluid based Navier–Stokes free surface flow model (Bradford, 2011).

3. Numerical solution

The finite volume approach is used to discretize Eqs. (2) and (8). The domain is divided into cube-shaped computational cells indexed with j, k, l and all dependent variables are defined as cell average values. ξ is in the direction of contiguous j indices, while η and σ are in the directions of k and l indices, respectively, as shown in Fig. 1.

Eq. (8) is solved for D as

$$A_{j,k}\frac{D_{j,k}^{n+1}-D_{j,k}^{n}}{\Delta t}+(D\bar{U})_{j+1/2,k}^{n+1/2}-(D\bar{U})_{j-1/2,k}^{n+1/2}+(D\bar{V})_{j,k+1/2}^{n+1/2} -(D\bar{V})_{j,k-1/2}^{n+1/2}=0 \tag{14}$$

where the superscript $n+1$ denotes the new time level, n the previous time level, $n+1/2$ is the predictor time level, and Δt is the time step. The depth-averaged fluxes, $D\bar{U}$, are computed by approximately solving the Riemann problem given by the reconstructed flow variables to the left and right of each cell face (Roe, 1981), which is summarized in Appendix A.

Eq. (2) are solved for $\mathbf{U}$ as

$$\frac{\mathbf{U}_{j,k,l}^{n+1}-\mathbf{U}_{j,k,l}^{n}}{\Delta t}+\frac{1}{A_{j,k}}\left(\mathbf{F}_{j+1/2,k,l}^{n+1/2}-\mathbf{F}_{j-1/2,k,l}^{n+1/2}+\mathbf{G}_{j,k+1/2,l}^{n+1/2}-\mathbf{G}_{j,k-1/2,l}^{n+1/2}\right) +\frac{\mathbf{H}_{j,k,l+1/2}^{n+1/2}-\mathbf{H}_{j,k,l-1/2}^{n+1/2}}{\Delta\sigma_l}-B_{j,k,l+1/2}(\mathbf{U}_{j,k,l+1}^{n+1}-\mathbf{U}_{j,k,l}^{n+1}) -B_{j,k,l-1/2}(\mathbf{U}_{j,k,l}^{n+1}-\mathbf{U}_{j,k,l-1}^{n+1})=\mathbf{Z}_{j,k,l}^{n+1/2}+\mathbf{P}_{j,k,l}^{n+1/2} \tag{15}$$

where

$$B_{j,k,l\pm1/2}=\frac{\nu_{j,k,l\pm1/2}}{D_{j,k}^2\Delta\sigma_l\Delta\sigma_{l\pm1/2}} \tag{16}$$

Note that vertical diffusion is integrated in time with the first order accurate, implicit Euler method. Bradford (2004) found that the implicit Euler method coupled with the neglect of diffusion in computing the predictor solution ($\mathbf{U}^{n+1/2}$), yielded the best combination of computational efficiency, accuracy, and robustness.